Stern-Brocot trees in spiking and bursting of sigmoidal maps

Joana G. Freire, Thorsten Pöschel and Jason A. C. Gallas

Institute for Multiscale Simulations, Friedrich-Alexander-Universität - 91052 Erlangen, Germany, EU and
Departamento de Física, Universidade Federal da Paraíba - 58051-970 João Pessoa, Brazil

Abstract – We study the global organization of oscillations in sigmoidal maps, a class of models which reproduces complex locking behaviors commonly observed in lasers, neurons, and other systems which display spiking, bursting, and chaotic sequences of spiking and bursting. We find periodic oscillations to emerge organized regularly according to the elusive Stern-Brocot tree, a *symmetric* and more general tree which contains the better-known *asymmetric* Farey tree as a sub-tree. The Stern-Brocot tree provides a natural and encompassing organization to classify nonlinear oscillations. The mathematical algorithm for generating both trees is exactly the same, differing only in the initial conditions. Such degeneracy suggests that the wrong tree might have been attributed to locking phenomena reported in some of the earlier works.

Introduction. – The study of sigmoidal maps has attracted increasing interest in recent years because they can reproduce all the complex behaviors commonly observed in systems like lasers, capable of displaying spiking, bursting, and chaotic spiking-bursting, as well as in neurons, which, in addition, can show subthreshold oscillations, tonic and phasic spiking, normal excitability, etc. The utility of sigmoidal functions was nicely described in the pioneering work by Rinzel [1], by Pinto and coworkers [2], in several works dealing with the fruitful maps introduced by Rulkov [3], and in other families of maps as surveyed recently in a comprehensive way by Ibarz *et al.* [4]. Although the name sigmoidal is not always explicitly mentioned, *e.g.*, in ref. [5], such behavior can be easily identified. When combined to form networks, large arrays of such maps can be used to investigate questions related with, *e.g.*, emergent complex neural dynamics and the activity patterns in the brain [6–8].

Motivated by all the aforementioned applications, our aim here is to show that spiking, bursting and periodic patterns generated by the paradigmatic sigmoidal family of maps emerge regularly organized according to a Stern-Brocot tree [9–15] an elusive and very general hierarchical tree that was recently identified in certain systems governed by differential equations [16,17]. The discovery of Stern-Brocot sequences in discrete-time mappings is very relevant because such maps allow one to bypass all numerical difficulties usually connected with the integration of differential equations and to explore with high-resolution

fine details about the hierarchical genesis and organization of oscillatory patterns and locking behaviors up to very high generations (see below). An interesting practical aspect of our work is that we classify periodic patterns directly from their period, without resorting to an intermediate torus as it is normally done. In fact, the most general mechanism for the Stern-Brocot sequence does not require any torus (*i.e.*, a pair of frequencies). This is also the case for the Farey tree as recognized long ago: "However, evidence for the tori is suggestive, not conclusive" [18]. As will be seen below, this important and almost forgotten caveat is borne out forcefully by the Stern-Brocot tree.

There are two strong motivations for studying sigmoidal maps and their Stern-Brocot organization of periodic patterns. One is the fact that the *symmetrical* Stern-Brocot tree provides a much more general framework than the better-known *asymmetrical* Farey tree and, in particular, contains it as a sub-tree [11–15]. The other motivation is that, being more general, the Stern-Brocot tree provides a natural and encompassing organization to classify stable nonlinear oscillations and locking phenomena for a broad class of systems. Surprisingly, the Stern-Brocot tree seems to have eluded detection in maps so far although, as shown below, they are not difficult to spot. Of course, this apparently unbalanced situation may be just a result of lack of familiarity with the more general tree. We hope our report here to help to cast a fresh light on this subject.

As is clear from the phase diagrams discussed below, the spiking ordering found for all members of the sigmoidal

familiy of maps (fig. 1) does not correspond to the ordering generated by the Farey tree but it is in perfect agreement with the integers in the Stern-Brocot sum tree (fig. 2). This "good" tree was devised independently in 1858 by Moritz Stern [9] and in 1861 by Achille Brocot [10]. Stern was a German mathematician and Brocot a French clockmaker. The latter used this tree to design systems of gears with a gear ratio close to some desired value by finding a ratio of numbers near that value. The Stern-Brocot and Farey trees are generated by exactly the same arithmetic principle. However, as abundantly discussed in the literature [12,13], Stern-Brocot trees are more general than Farey trees and include them as sub-trees.

The Stern-Brocot sequence differs from the Farey sequence in two basic ways [12]: it eventually includes all positive rationals, not just the rationals within the interval $[0, 1]$, and at the n-th step all mediants are included, not only the ones with denominator equal to n. The Farey sequence of order n may be found by an in-order traversal of the left sub-tree of the Stern-Brocot tree, backtracking whenever a number with denominator greater than n is reached. "*But we had better not discuss the Farey series any further, because the entire Stern-Brocot tree turns out to be even more interesting.*" [12].

As mentioned, the construction of both trees obeys exactly the *same arithmetical procedure* [11–15]. Since there are abundant reports of observations of the Farey tree in the literature and virtually none of the Stern-Brocot tree, it is possible that the degenerate arithmetic process underlying both trees may have resulted in the Farey tree being identified far too often, particularly in situations where the number of accessible patterns is limited. We hope our work to draw attention for the necessity of a careful re-examination of the distribution of frequency-locking plateaus in earlier works.

The sigmoidal family of maps. – The sigmoidal family of maps is defined by the recurrence relation

$$x_{t+1} = A[a - s(bx_t)] + Bx_t, \qquad (1)$$

where x_t is a real variable and A, B, a, b are freely tunable real parameters whose specific meaning depends of the sigmoidal function $s(x)$, an S-shaped function (fig. 1). Typical examples of maps belonging to the sigmoidal family are the following:

$$s_1(x) = \mathrm{erf}(x), \qquad s_2(x) = \tanh(x), \qquad (2a)$$

$$s_3(x) = \frac{x}{\sqrt{1+x^2}}, \qquad s_4(x) = -1 + \frac{2}{1+e^{-x}}, \qquad (2b)$$

$$s_5(x) = \frac{2}{\pi}\arctan(x), \quad s_6(x) = \frac{x}{1+|x|}. \qquad (2c)$$

The map with $s_2(x)$ plays the key role as the activator in certain Hopfield neural networks [19–22]. The map with $s_5(x)$ has a practical application in economy
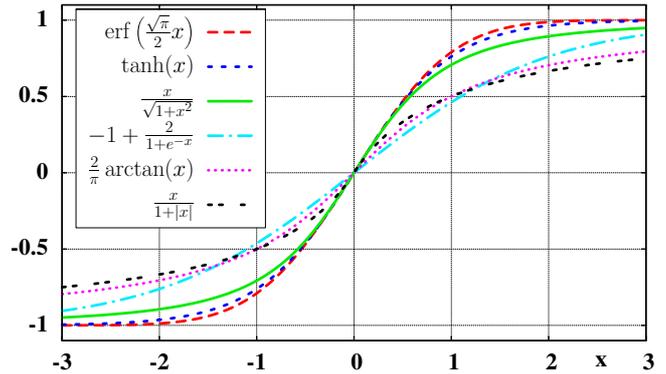
Fig. 1: (Color online) Comparison of six representative sigmoidal functions $s_i(x)$ defined in eqs. (2a)–(2c). Detailed phase diagrams for three of them are presented in figs. 3–5 (see text).

where it describes a cobweb model with adaptive expectations [23,24]. The other maps are standard representations of additional sigmoidal functions that, as shown in figs. 3–5, share the properties that characterize the whole sigmoidal class. An additional sigmoidal closely resembling $s_1(x)$ is the Gudermannian function $\mathrm{gd}(x) = 2\arctan(\exp(x)) - \pi/2$. Following earlier work [24] and with no loss of generality, we fix $A = 1$ and $B = 0.7$ in eq. (1). In fig. 1 we compare the distinct functions $s_i(x)$ in eqs. (2a)–(2c). As the figure shows, these sigmoids look relatively similar (but far from identical) and this similarity bespeaks the isomorphism observed in their behaviors in real-life applications [21,22]. In fact, they all can be shown to share isomorphic dynamical behaviors after simple affine transformations [25]. Also of interest to us is the fact that such remarkable families of maps can be obtained abundantly around *periodicity hubs* [26,27], the exceptional points in dissipative flows like electric discharges, lasers and chemical oscillators, etc. [28–30].

With the advent of fast throughput processors it is becoming increasingly feasible to contrast the control parameter space of flows and maps, determining their detailed structure, sorting out their differences and similarities. It is also possible to assess the validity of the models being used nowadays and the adequacy of parameter sets normally extracted phenomenologically or introduced in an *ad hoc* manner. Of special interest to us is to see whether or not specific characteristics normally found in stability diagrams may be used to infer if the underlying dynamics is governed by a flow (continuous time dynamical system) or by maps (discrete time systems). For flows, it is already known that systems governed either by ordinary differential equations (ODEs) or by the much more complicated delay-differential equations (DDEs) display similar overall distributions of periodicity islands but with rather distinct inner arrangements, a fact that should allow one to discriminate between ODE and DDE dynamics in experimentally constructed phase diagrams [31]. The
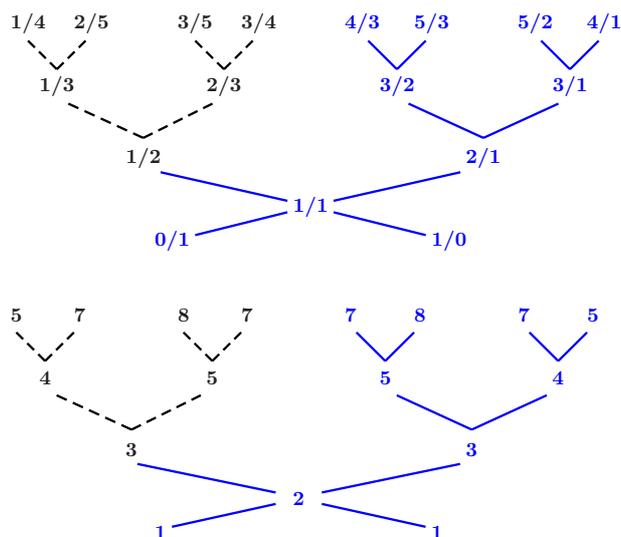
Fig. 2: (Color online) The first few generations of the infinite Stern-Brocot tree (top), grown as usual [11–15] by arranging reduced fractions in the $[0,1]$ interval into n-th–order sequences. The tree of periods (bottom) is derived from the Stern-Brocot tree by adding the numerator and denominator of the fractions. The asymmetric Farey sub-tree is indicated by dashed lines. Only the symmetric sequence of periods of the Stern-Brocot tree reproduces the hierarchies of periods observed for the generic systems of figs. 3–5.

Fig. 3: (Color online) Phase diagrams illustrating the Stern-Brocot symmetric distribution of periodicity phases with respect to the line $a = 0$ for $s_5(x) = \frac{2}{\pi} \arctan(x)$. (a) Global view of the $a \times b$ space. The four white boxes are shown magnified in fig. 5. (b) Enlargement of the bottom part of (a), showing details of the first few larger domains of periodicity. Numbers refer to the period determined for the map and obey the Stern-Brocot sequence given in fig. 2. Each panel shows $2400^2 = 5.76 \times 10^6$ parameter points.

availability of detailed stability diagrams for flows makes it natural to re-assess the completeness and scope of analogous diagrams generated by maps.

Stern-Brocot and Farey sequences. – While performing extensive numerical simulations we noticed that, upon variation of the control parameters, the oscillatory patterns of sigmoidal maps invariably emerged regularly organized according to a distinctive and elusive sequential way known as the *Stern-Brocot tree* [11–15], described in the introduction.

As already mentioned, the nowadays well-established organization believed to underly complex oscillatory patterns across all natural sciences is the so-called *Farey tree* or, equivalently, Farey sequence [11–15]. Therefore, it is natural to ask about the relation between the Farey and the Stern-Brocot trees. In a Farey tree, the sequence of order n is defined as the sequence of completely reduced fractions between 0 and 1 which, when in lowest terms, have denominators less than or equal to n, arranged in order of increasing size. Each Farey sequence starts with the value 0, denoted by the fraction $0/1$, and ends with the value 1, denoted by the fraction $1/1$ (terms which are not always shown as belonging to the sequence).

The construction algorithm for the Farey and Stern-Brocot trees is summarized in fig. 2. The Farey tree is indicated by the dashed lines. As it is clear from the figure, the Farey tree represents less than half of the Stern-Brocot tree. Moreover, as discussed abundantly in the literature, the Stern-Brocot is a *symmetric* tree which contains the *asymmetric* Farey tree as a sub-tree [11–15]. In other words, the Stern-Brocot tree is a far more general tree. The lower panel of fig. 2 presents the tree of periods which is obtained from the Stern-Brocot tree by adding the numerator and denominator of each fraction. This sequence of periods is what is observed when recording the unfolding of the periodicity while tuning control parameters.

The Stern-Brocot and the Farey tree have something quite remarkable in common: *both trees are generated by the same mathematical procedure*, referred to as the "Farey arithmetic" [11,12,14,15]. The only difference between them are the initial conditions used to begin the construction of the tree. Since both trees are generated by precisely the same algorithm, in practical applications it is not possible to discriminate them by considering just a small number of generations. In experiments one does not usually starts to generate the tree from the very beginning, but only checks if a few periodic patterns obey the Farey arithmetics. Obviously, observation of just a few periodic patterns that obey the Farey arithmetics is not enough evidence to conclusively discriminate both trees.

(a) $s_2(x) = \tanh(x)$

(b) $s_4(x) = -1 + \frac{2}{1+e^{-x}}$

(c) $s_5(x) = \frac{2}{\pi}\arctan(x)$
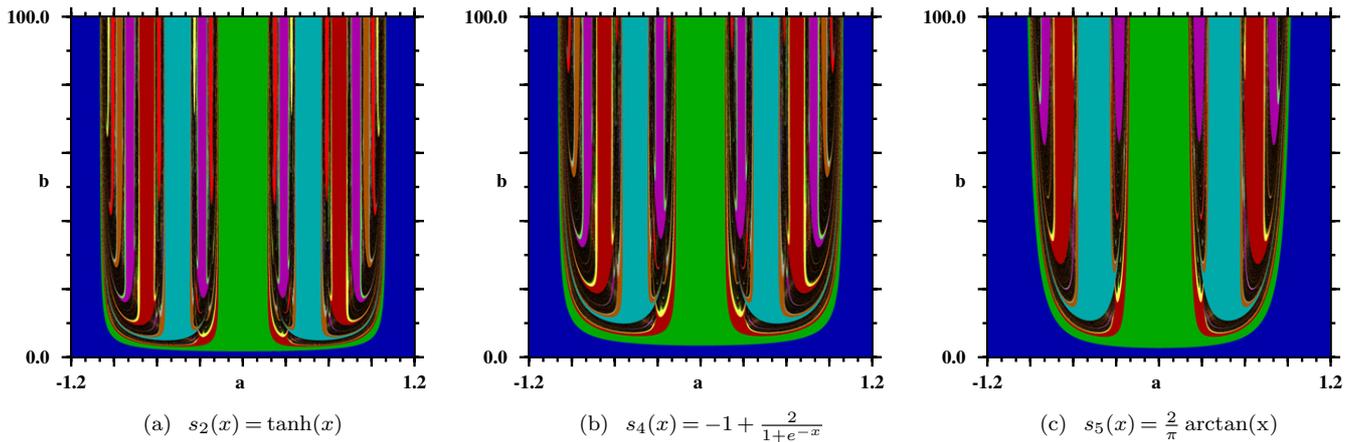
Fig. 4: (Color online) Comparison of the Stern-Brocot distribution of periodic phases for sigmoids of decreasing steepness, from left to right. A decrease in the steepness has an effect similar to zooming in at the bottom of the tree. While the distribution of periodic and chaotic phases for the sigmoids looks globally identical, differences exist on a fine scale. Colors are as defined in fig. 3.
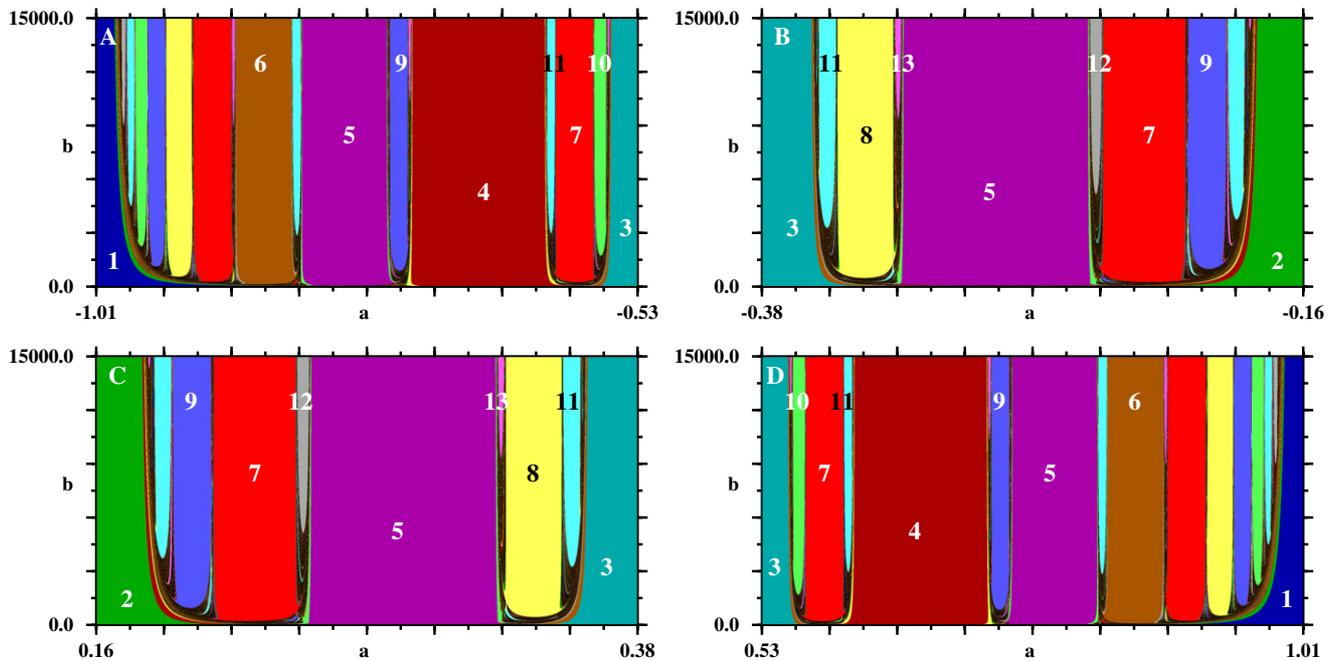
Fig. 5: (Color online) The first six generations of the Stern-Brocot tree. Numbers refer to the period. These panels are magnifications of the white boxes in fig. 3(a) and each one displays the analysis of $2400^2 = 5.76 \times 10^6$ parameter points. Colors are as defined in fig. 3.

Phase diagrams. – We now present phase diagrams depicting the distinct periodic and chaotic stability phases computed for a representative selection of sigmoidal maps, defined by eqs. (2a)–(2c). Such diagrams were obtained by determining the asymptotic periodicity (or lack of it) for the map for each point of a finely spaced mesh in the $a \times b$ parameter plane. Then, by attributing different colors to the distinct dynamical states it is possible to obtain very detailed charts characterizing how the periodic and aperiodic oscillations are distributed in the control parameter plane, together with the size and shape of each individual dynamical phase. The number of periodic

phases found is normally high so that parameter regions turn out to be quite complex mosaics displaying graphically an intricate chart of phases resulting from the different periodic oscillations. Our diagrams show 14 distinct shadings to represent the 14 lowest periods, as indicated by the colorbar. Higher periods are plotted recycling the 14 basic shadings "mod 14". Black represents chaos, *i.e.*, represents parameters leading to oscillations with no numerically detectable periodicity [25]. Comparing figs. 2 and 3 one easily realizes that the sequence of periods of the map emerge organized according to the Stern-Brocot tree.

Figure 3 shows a typical example of a diagram classifying periodic and non-periodic oscillations supported by the sigmoidal map, eq. (1), with $s_5(x) = \frac{2}{\pi}\arctan(x)$. This diagram reveals an unambiguous organization into a Stern-Brocot tree which is representative of what we find for all other functions in the sigmoidal class. Noteworthy in fig. 3 is that the distribution of periodic and chaotic phases is symmetric with respect to the central period-2 domain, a symmetry obviously not present in the Farey tree. Furthermore, although generated here for discrete-time dynamics, the typical phase diagrams found for maps agree very well with those obtained for rather more complex models governed by ordinary differential equations [16,17]. Similarly to what happens for differential equations, the generic unfolding of periodicities in the sigmoidal maps starts with a $1 \to 2$ period-doubling. The central period-2 phase contains two symmetrically located "armpits", each one containing its own period-doubling route to chaos and an infinite alternation of periodic and chaotic phases "embedded" in its armpits. The largest periodic structure inside the chaotic phases in each of the period-2 armpits is a period-3 phase, each one containing its own pair of armpits. The largest periodic structures inside the chaotic phase of the period-3 armpits are period-4 and period-5 phases, as indicated by the numbers. And this unfolding repeats *ad infinitum*, with the periods following the Stern-Brocot sequence. Note that only the Stern-Brocot tree is capable of reproducing the symmetric cascading produced by the maps.

Figure 4 presents a comparison of the periodic and chaotic phases for distinct sigmoidal functions making evident their great structural similarity. The figure shows clearly that to decrease the steepness of the sigmoids is equivalent to zooming into the lower part of the phase diagram. This means that the higher the steepness, the higher is the number of generations that are visible inside a constant window of parameters. As fig. 4 shows, periodic and chaotic phases get compressed very strongly as the periodicity grows.

To identify unambiguously the characteristic symmetry of the Stern-Brocot tree we magnify specific portions of the phase diagrams. For instance, fig. 5 shows magnifications of the four whites boxes seen in fig. 3(a). Such magnifications corroborate that the periodic oscillations perfectly follow the Stern-Brocot tree up to the 6th generation, a quite high number of generations that is not usually reproduced in the literature, being particularly difficult to follow experimentally. We checked the occurrence of several generations by further magnifications (not shown). Once more, we recognize that only the Stern-Brocot tree correctly reproduces the symmetric unfolding of the periodicity depicted in figs. 4 and 5.

Conclusions. – In summary, we find that the most general and encompassing natural organization of locking phenomena is symmetric in the period of oscillation and corresponds to the organization displayed by a Stern-Brocot tree. The considerations leading to this result do not involve a torus but, instead, are based on the direct classification of the periodicity of the physical oscillations observed, not on secondary quantities derived from them. Since Farey and Stern-Brocot trees are generated mathematically by exactly the same arithmetical procedure, it may be hard (not to say impossible) to correctly distinguish them from just a partial analysis based on relatively small parameter intervals or in the consideration of just a limited number of periods. Furthermore, previous analysis done without taking into account the complete symmetry of the underlying tree could be incorrect. Thus, we believe to be likely to find in the current literature systems improperly described as organized into asymmetric Farey trees while, in fact, their organization corresponds to the symmetric Stern-Brocot tree. Of course, there is no reason to believe that every sequence of periods observed in natural phenomena must necessarily involve the Stern-Brocot tree. Be it as it may, we hope our results to draw attention to the need of great care when asserting the nature of sequences of periods. Due to its full generality, the Stern-Brocot tree provides a rather natural scenario for classifying the unfolding of stable periodic oscillations for a broad class of phenomena. We believe the Stern-Brocot tree to provide a truly universal classification for periodic oscillations. As happened for the Farey sub-tree, other scenarios are likely to be just sub-trees of the more general Stern-Brocot tree. We hope the results presented here to contribute to the experimental discovery of the more general and symmetric organization of locking phenomena in the near future.

$$* * *$$

REFERENCES

[1] RINZEL J., *Bursting oscillations in an excitable membrane model*, in *Lecture Notes in Mathematics*, edited by SLEEMAN B. D. and JARVIS R. J., Vol. **1151** (Springer) 1985, pp. 304–316; *A formal classification of bursting mechanisms in excitable systems*, in *Lecture Notes in Biomathematics*, edited by TERAMOTO E. and YAMAGUTI M., Vol. **71** (Springer, Berlin) 1987, pp. 267–281.

[2] PINTO R. D., VARONA P., VOLKOVSKII A. R., SZÜCS A., ABARBANEL H. D. I. and RABINOVICH M. I., *Phys. Rev. E*, **62** (2000) 2644.

[3] RULKOV N. F., *Phys. Rev. E*, **65** (2002) 041922; SHILNIKOV A. L. and RULKOV N. F., *Phys. Lett. A*, **328** (2004) 177.

[4] IBARZ B., CASADO J. M. and SANJUAN M. A. F., *Phys. Rep.*, **501** (2011) 1.

[5] MEDVEDED G. S. and ZHURAVYTSKA S., *Biol. Cybern.*, **106** (2012) 67.

[6] CHIALVO D.R., *Nat. Phys.*, **6** (2010) 744.

[7] BRANDT S.F., PELSTER A. and WESSEL R., *EPL*, **79** (2007) 38001.

[8] KUVA S. M., LIMA G. F., KINOUCHI O., TRAGTENBERG M. H. R. and SILVA A. C. R., *Neurocomputing*, **38-40** (2001) 255.

[9] STERN M.A., *J. Reine Angew. Math.*, **55** (1858) 193.

[10] BROCOT A., *Revue Chronométrique, Journal des horlogers, Scientifique et Pratique*, **3** (1861) 186.

[11] HARDY G. and WRIGHT E., *An Introduction to the Theory of Numbers* (Clarendon, Oxford) 1979.

[12] GRAHAM R., KNUTH D. and PATASHNIK O., *Concrete Mathematics*, 2nd edition (Addison-Wesley, New York) 1994.

[13] BACKHOUSE R. and FERREIRA J. F., *Sci. Comput. Prog.*, **76** (2011) 160.

[14] BONANNO C. and ISOLA S., *Colloq. Math.*, **116** (2009) 165.

[15] GUTHERY S. B., *A Motif of Mathematics: History and Applications of the Mediant and the Farey Sequence* (Docent Press, Boston) 2010.

[16] FREIRE J. G. and GALLAS J. A. C., *Phys. Chem. Chem. Phys.*, **13** (2011) 12191; *Phys. Lett. A* **375** (2011) 1097.

[17] MARSZALEK W., *Circ. Syst. Signal Process.*, **31** (2012) 1279; PODHAISKY H. and MARSZALEK W., *Nonlinear Dyn.*, **69** (2012) 949.

[18] MASEŁKO J. and SWINNEY H. L., *J. Chem. Phys.*, **85** (1986) 6430.

[19] HUANG W. Z. and HUANG Y., *Int. J. Bifurcat. Chaos*, **21** (2011) 885.

[20] PÖSCHEL T. and GALLAS J. A. C., in preparation.

[21] MENON A., MEHROTRA K., MOHAN C. K. and RANKA S., *Neural Netw.*, **9** (1996) 819.

[22] MITCHELL T., *Machine Learning* (McGraw Hill, New York) 1997.

[23] HOMMES C. H., *J. Econ. Behav. Org.*, **24** (1994) 315.

[24] GALLAS J. A. C. and NUSSE H. E., *J. Econ. Behav. Org.*, **29** (1996) 447.

[25] GALLAS J. A. C., *Phys. Rev. Lett.*, **70** (1993) 2714; *Physica A* **202** (1994) 196; *Appl. Phys. B* **60** (1995) S-203.

[26] BONATTO C. and GALLAS J. A. C., *Phys. Rev. Lett.*, **101** (2008) 054101; *Philos. Trans. R. Soc. London, Ser. A* **366** (2008) 505.

[27] RAMIREZ-AVILA G. M. and GALLAS J. A. C., *Phys. Lett. A*, **375** (2010) 143; *Rev. Boliv. Fis.* **14** (2008) 1.

[28] GALLAS J. A. C., *Int. J. Bifurcat. Chaos*, **20** (2010) 197.

[29] VITOLO R., GLENDINNING P. and GALLAS J. A. C., *Phys. Rev. E*, **84** (2011) 016216.

[30] BRAGARD J., PLEINER H., SUAREZ O. J., VARGAS P., GALLAS J. A. C. and LAROZE D., *Phys. Rev. E*, **84** (2011) 037202; LAROZE D., BECERRA-ALONSO D., GALLAS J. A. C. and PLEINER H., *IEEE Trans. Magn.*, **48** (2012) 3567.

[31] JUNGES L. and GALLAS J. A. C., *Phys. Lett. A*, **376** (2012) 2109; *Opt. Commun.* **285** (2012) 4500.